Research Article
Open Access

Corrosion behavior of Al-Fe alloy metastable phases produced by laser surface remelting technic

Abstract

Laser surface remelting (LSR) treatment was performed to Al–2.0 wt.% Fe alloy with a 2 kW Yb-fiber laser (IPG YLR-2000S). Characterization of substrate and laser-treated material were executed using different techniques, i.e., microstructure was analyzed by optical microscope, SEM, low-angle X-ray diffraction (LAXRD) and corrosion test was made in aerated solution of 0.1 mol/L of H_2SO_4 at 25°C. As result was shown micrograph of LSR-treated material, it displaying a fine cellular structure, as well as existence of certain nano-porosities and similar a nano-dendritic growth was observed too. Characteristic of melted zone was constituted of metastable phases according to x-rays result and corrosion behavior as a result of LSR-treated sample, which it was shown to be more resistant to corrosion than untreated sample. A comparative study was carried out of cyclic polarization of the laser-treated and untreated samples, demonstrating that LSR-treated sample propitious the passivity on the surface and so reduced the corrosion phenomena, wherefore, this type of laser-treated alloy can be applied in the aerospace, aeronautic, automobilist industries and implant material in humans.

Keywords: Al–2.0 wt.% Fe alloy, laser-treated, microstructure, low-angle X-ray diffraction, cyclical polarization

Volume 4 Issue 3 - 2018

Moises Meza Parionaa, Katieli Tives Micene, Alfredo Jose Zaraa

Graduate Program in Engineering and Materials Science, State University of Ponta Grossa, Brazil

Correspondence: Moises Meza Parionaa, Graduate Program in Engineering and Materials Science, State University of Ponta Grossa (UEPG), Ponta Grossa 84010-919, PR, Brazil, Email mmpariona@uepg.br

Received: August 30, 2017 | **Published:** June 15, 2018

Introduction

The aluminium oxide or alumina has important properties, because the alumina is produced during laser surface remelting (LSR) treatment, and this technique does not suit within the traditional techniques, it is a modern technique that is being used recently, therefore it is important to focus on this work. As well, the authors Nakajima et al.,[1] studied the formation behavior of the anodic alumina nanofibers via constant voltage pyrophosphoric acid anodizing. They have discussed extensively on aluminum oxide films fabricated via anodizing in various electrolyte solutions, furthermore, they affirm that this technique have been widely investigated in various applied sciences and technologies due to their characteristic nanomorphologies and chemical/physical properties. In general, anodic aluminium oxide can be classified into two different types, as follows: barrier and porous oxides. Barrier oxides have been widely used for electrolytic capacitor applications due to their high dielectric property. Anodic porous alumina has been widely used for various nanoapplications, such as optical devices and nanotemplates.

Laser surface treatment of metals is a process where a small surface volume of materials is melted instantly by a laser beam and rapidly cooled, thereby producing very fine microstructure with an improved wear and corrosion resistance. Laser surface melting (LSM) was reported by Lee et al.,[2] to improve the corrosion resistance of Zircaloy-4 in acid solution.

In this study the microstructural and corrosion resistance analysis of hypereutectic Al–2.0 wt.% Fe alloy LSR-treated was performed and this was aim of this research, where the substrate and laser-treated material were characterized using different techniques, i.e, the microstructure was analyzed by optical microscope, SEM, low-angle X-ray diffraction (LAXRD) analysis and corrosion test was performed in aerated solution of 0.1 mol/L of H_2SO_4 at 25°C. In electrochemical study, following tests were carried out, open circuit potential, polarization resistance, corrosion current, determination of the corrosion rate and finally cyclical polarization for the untreated and laser-treated samples. Importance of this research is due that LSR-treated alloy presented metastable phases, which between them, what are of greater importance are alumina and nitrite, presence of a fine cellular structure and the existence of certain nano-porosities, a high corrosion resistance and a large plateau of passive zone, and therefore this type of laser-treated alloy can be applied in the aerospace, aeronautic and automobilist industries.

Materials and methods

Experimental characterization

Material

Al–2.0 wt.% Fe alloy was prepared with commercially pure raw materials, being that the aluminium has 99.76% purity, containing 1.54 wt.% of iron, and other elements with quantities below 50 PPM. Casting assembly used in solidification experiments consists of a water-cooled mold and the heat was extracted only from bottom, promoting vertical upward directional solidification. This apparatus was used to obtain cylindrical casting, with dimensions of 6 cm diameter and 10 cm length. Preparation of samples for analysis consisted in sectioning the cylindrical casting into several longitudinal slices, and milling surfaces to improve parallelism. Each piece was sanded with 1200# SiC s and paper and then sand-blasted was applied to reduce the surface reflectivity, thus increasing the laser energy absorption coefficient.

Laser surface remelting treatment specifications

Laser surface remelting (LSR) treatment was performed with a 2 kW Yb-fiber laser (IPG YLR-2000S) that operates at wavelength of 1.07µm. The laser beam is coupled to a 160 mm focusing lens (optical head). For this optical system the focused beam diameter was 100 um. The laser output power was 600 W and the scanning speed was 40mm.s^{-1}. For this experiment, the sample was positioned 3 mm above the focus (out of focus), which results in a 600µm diameter laser beam, which was designed by Riva et al.[3] Assuming a near Gaussian

laser beam profile, the power density was 21.2x104W.cm^{-2}, which were studded by Steen and Mazumde[4] Average distance between weld fillets was 300µm. The device operated without shielding gas in order to increase between the metal and the ambient gas which contributes to formation of a passivation oxide layer on the substrate surface.

After laser processing, different regions were identified in the sample cross-section, through SEM micrographs analysis: laser melted zone (LMZ), interface between the treated region and the substrate, and unaffected region (substrate), which was studied by Pariona et al.[5] On the sample surface there is two distinct regions: region on the weld fillet and region between the weld fillets, this has been discussed and studied by Pariona et al.[5,6]

Characterization techniques

The substrate and laser-treated material characterization was performed using different techniques, therefore, the microstructure was analyzed by a Shimadzu SSX-550 scanning electron microscope (SEM) and an Olympus BX-51 optical microscope (OM) with a Q-Color 3 digital camera for image capture. SEDS-500 energy dispersive spectroscopy (EDS) equipment was used for semi-quantitative analysis and it was coupled to SEM. As well, low-angle X-ray diffraction (LAXRD) analysis were recorded at a scan speed of 0.2°min^{-1}, using a Lab XRD-6000 diffractometer (minimum detection >1%). The corrosion test was performe in aerated solution of 0.1M H_2SO_4 at a temperature of 25°C±0.5°C. Working electrodes of surface-treated and untreated samples were prepared with epoxy resin to expose a top surface. Corrosion potentials (Ecor) were measured using Autolab PGSTAT 30 potentiostat system connected to a microcomputer. Samples were cut with diamond disk. For the cross-section analysis them were sanded (600 up to 1200#), then polished with diamond paste (1µm) and colloidal silica. The chemical attack with 0.5% HF was also made on these samples for analysis microscopic.

Results and Discussion

Electrochemical behavior study of samples

To better understand tcorrosion process that occurs of laser-treated Al–2.0 wt.% Fe alloy, an samples micrographs study in both were done, as much on the surface and as well as in the cross-section were executed, details of changes that suffers when was subjected to LSR-treated sample and whose results will be shown to follow. Soon it will be discussed influence of micrograph on result of electrochemical study. As well, in electrochemical study, following tests were carried out, among them, the open circuit potential (OCP), polarization resistance, corrosion current (Icor), determination of the corrosion rate and finally cyclical polarization for untreated and laser-treated samples.

Microstructural study

In this work, the untreated surface of Al–2.0 wt.% Fe alloy was covered with an arrangement of multiple weld fillets, in order to analyze this treatment, micro-porosity has been observed on the laser-treated sample surface and more preferably at on the weld fillet region. Besides that, the protuberance on this surface was observed, which corresponds to on the weld fillet region, a similar result of this microstructure was given by Sun et al.[7] Figure 1 shows the specimen cross-section analysis, where three different regions are observed: the melted zone, interface between treated region and substrate, and specifically the substrate.

The first region (Figure 1A) is characterized by a fine cellular structure, as well as, existences of certain nano-porosities and also in this region, presence of protuberances is observed, which they corresponds to between weld fillets region. According to Pariona et al.,[8] presence of the protuberances is more perceptible in Al–1.5 wt.% Fe alloy than Al–2.0 wt.% Fe alloy. In Figure 1a are observed, the overlapping lines and being more magnified in Figure 1b, these highlighted lines are due to overlapping of consecutive weld fillets, this phenomenon was also observed by the Yan et al.,[9] they have verified, which the melt pools are overlapping one with other.

These overlapping lines are most notorious in Al–2.0 wt.% Fe alloy that in Al–1.5 wt.% Fe alloy.[5,6,8] Here it should be pointed, despite that the laser beam velocity was remained same at 40 mm/s, for the treatment of hypoeutectic Al–1.5 wt.% Fe alloy and to hypereutectic Al–2.0 wt.% Fe alloy, because, difference of Fe concentration had significant influence on overlapping lines characteristic, in the melted zone region. In order to clarity, the region of Figure 1B has been still more magnified as shown in Figure 1C, where is observed a similar to a nano-dendritic growth, possibly following the direction of thermal gradient and however, around the overlapping lines there are a high concentration of nano-porosity, that it can be noticed. However, in the region between the overlapping lines in Figure 1D, with high magnification is observed a fine cellular structure with columnar growth, this result is similar to study realized by Olakanmia et al.,[10] and Fu et al.[11]

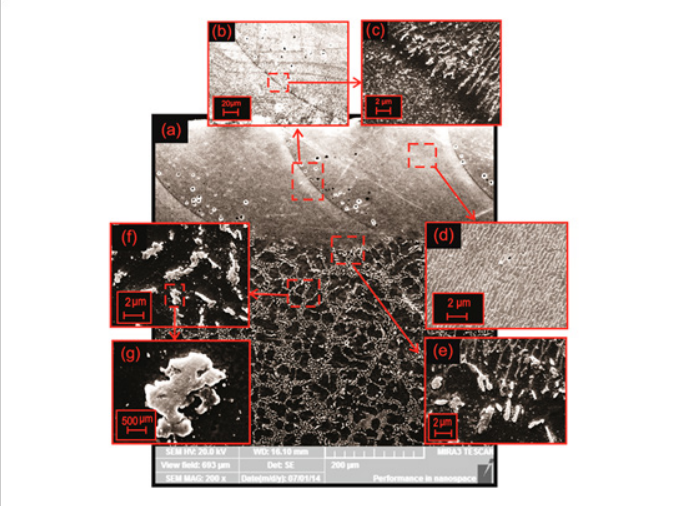

Figure 1 SEM image in the LSR-treated cross-section of Al–2.0 wt.% Fe alloy. (a) The melted zone and substrate region, (b) the overlapping of consecutive weld fillets, (c) magnified region of (b), (d) magnified of the laser melted zone, (e) the interface between treated region and the substrate, (f) magnified of the substrate region and (g) higher magnified of (f).

On the other hand, in interface between the treated region and the substrate was not observed clearly feature of the heat affected zone (HAZ), it has been studied by other authors, between them, Bertelly et al.,[12] these authors have affirmed for low Fe concentration does not appear the HAZ. This region was magnified in Figure 1E, which shown a structure with growth similar to nano-dendritic, following the direction of thermal gradient to substrate region. Specifically in the substrate region of Al–2.0 wt.% Fe alloy, the micrograph of this region is similar to Al–1.5 wt.% Fe alloy, which is constituted by grain boundaries, as such has been studied by Pariona et al.,[8] these authors confirmed the matrix with second-phase particles, which precipitated on the grain-boundary of substrate, which may be verified in Figure

1A. This region has been magnified as such is shown by SEM in Figure 1, where it is clearly shown the treated and untreated regions. Moreover, this region was higher magnified as shown in Figure 1F, where are observed the alloy matrix (green region) and intermetallic phases (white region) and even with higher magnified can be seen in Figure 1G, where it is constituted by the intermetallic Al_3Fe phase, this results was confirmed by X-ray microanalysis studies (next section).

Characteristic of the melted zone is mainly due to the high cooling rate imposed during RSL-treatment, ASM[13] author asserted, in low-energy-input laser welding process, it can induce a very high cooling rate (1000-10000°C.s^{-1}) and laser surface remelting may produce an even higher cooling rate. For this motive, the melted zone can be constituted of metastable phase.

Low-angle X-ray diffraction (LAXRD) analysis

Phases formed on the LSR-treated surface and untreated samples were analyzed using LAXRD technique, as described in Materials and Methods section.

LAXRD analysis in Figure 2 revealed presence of Al_2O_3 and AlN phases in most of diffraction peaks of treated sample figure shows the diffraction peaks of the untreated and treated samples. As can be seen, intensity of the diffraction peaks of the treated sample is higher than the untreated sample, this may be due to new phase presence, among them AlN phase, which is consistent with findings reported by Bian et al.,[14] and Pariona.[8]

In this study, high energy applied in laser-treatment, allied to fact that it was carried out in a suitable environment, for formation of oxides and nitrides, favored the characteristics of high hardness, wear and corrosion resistance of LSR-treated samples in acidic or alkaline media, as has also been reported by Patnaik.[15]

In addition to simple metal phases shown in Figure 2, intermetallic metastable phases were also identified, such as, AlFe, $AlFe_3$ and $Al_{13}Fe_4$. Formation of these phases is important because they determine the roughness, hardness and corrosion behavior of the treated layer. Other authors have also made this type of analysis, among them, Bertelli et al.,[12] Pariona et al.,[8] and Gremaud et al.[16]

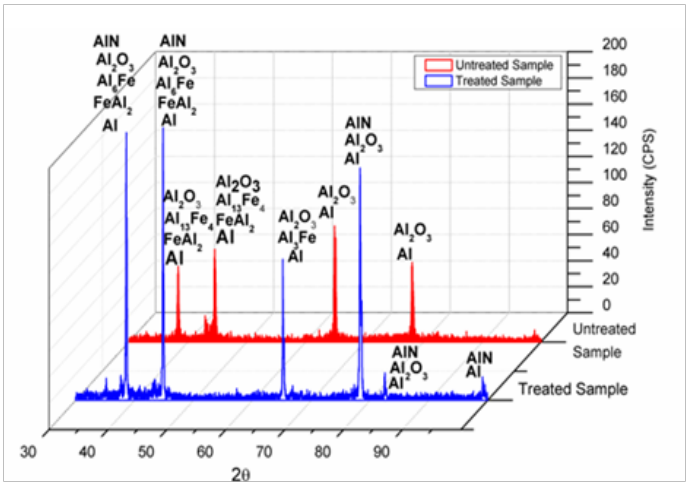

Figure 2 LAXRD profiles on the Al–2.0 wt.% Fe alloy LSR-treated surface.

Corrosion behavior

Polarization resistance of laser-treated and untreated samples

Figure 3 shows the current density behavior, after a linear polarization ±10mV around of Al–2.0 wt.% Fe alloys corrosion potential, for LSR-treated and untreated samples, where the red line represents results for the treated sample, while, the dark color curve is to the substrate without treatment.

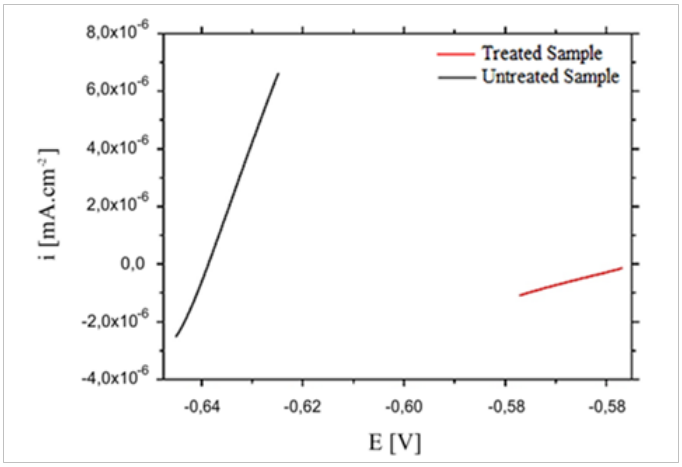

Figure 3 Linear Polarization near of Ecorr for electrodes of treated and untreated samples of Al–2.0 wt.% Fe alloys versus ECS in 0.1 mol/L H_2SO_4 at 25°C.

Micropolarization of ±10 mV around corrosion potential promotes a perturbation in equilibrium potential, giving appearance of an anodic and cathodic current in the electrochemical cell circuit. This technique of electric current versus applied potential was conducted to laser-treated and untreated samples, and result is shown in Figure 3. Inverse slope of the line in Figure 3 allows to determine the polarization resistance of system, that is associated with charge transfer processes in the interface metal/oxide/electrolyte solution, therefore, microstructural characteristic of laser-treated sample, definitely influences the polarization resistance (Rp) in relation to untreated substrate. Inverse of the slope of Figure 3 allowed determined Rp for both types electrodes, according to analysis, one can see that the line corresponding to the substrate has a slope greater than the laser-treated sample, i.e, at the substrate can be perceived that the current density suffers a greater variation, consequently generates a lower Rp for the substrate. Data obtained confirm this fact, for the laser-treated sample was determined, RP equal a 22.1 K ohms, however, for the substrate was 2.08 K ohms, which means an increase of about 11 times for the laser-treated sample relative to the untreated sample, this result showed that the metal/solution interface has peculiar behavior, consequently, the polarization resistance has direct impact on corrosion rates on the exposed surfaces with sulfuric acid. Second Li et al.[17] the highest polarization resistance of treated sample is related to greater difficulty of charge transfer at interface between the electrode and the electrolyte solution, possibly indicating the formation of new phases on the treated surface, implying directly on corrosion resistance of material. Also, a similar result for Al–1.5 wt.% Fe alloy was widely discussed by Pariona et al.,[8] and Peyre et al.,[18] discussed a similar result for 316L steel.

Citation: Parionaa MM, Micene KT, Zaraa AJ. Corrosion behavior of Al-Fe alloy metastable phases produced by laser surface remelting technic. *Adv Tissue Eng Regen Med Open Access*. 2018;4(3):57–62. DOI: 10.15406/atroa.2018.04.00079

Corrosion resistance, Tafel plots for LSR-treated and untreated alloy

Figure 4 shows the open-circuit corrosion potentials of the: laser-treated surface, as-received Al–2.0 wt.%Fe sample and substrate. Open circuit potential was recorded continuously for 1 h after immersion using a saturated calomel (SC) reference electrode. In Figure 4 is noted that potential corrosion, which to decrease as a function of time, being more evident for the substrate, around 700 s the substrate reaches stability and after 2000 s the potential tends to increase slightly, however, LSR-treated sample decreases more slowly when time increases, and after 2000 s regrowth is slower still. For longer times can will predict and that these potentials can will be find. Comparing two curves (Figure 4), the corrosion potential of LSR-treated alloy was increased by up to 8 mV, after 1 h in relation to the untreated material, which can be noticed in this figure, therefore, the laser-treated alloy became nobler than the untreated one. A similar result to this work was discussed by Khalfaoui et al.,[19] these same authors have also shown, when the laser-treated and untreated samples were exposed in a corrosive solution for 2 h, several corrosion pits were observed in the untreated surface while the laser-treated layer was unaltered. This proves that the sample LSR-treated is more resistant to corrosion than the untreated sample. Also the authors Pariona et al.,[8] showed a similar study for Al–1.5 wt.% Fe alloy.

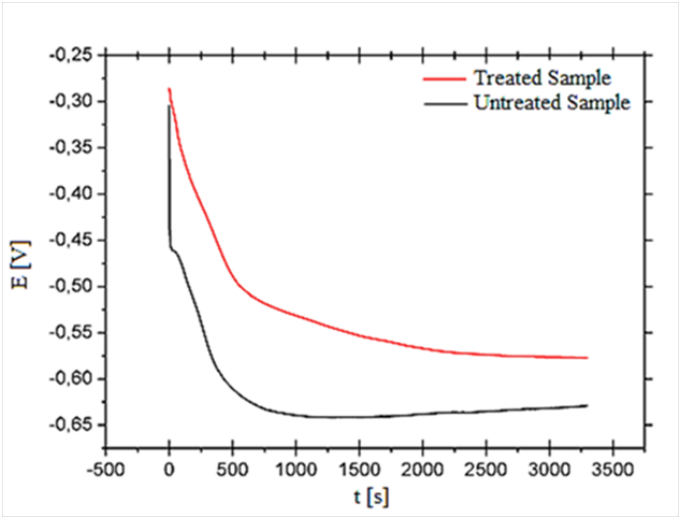

Figure 4 Evolution of open-circuit potential of Al 2.0 wt.% Fe alloy for LSR-treated and untreated samples, during immersion in 0.1 mol/L of H_2SO_4 at 25°C.

The anodic polarization curves are shown in Figure 5, where a confrontation was made between curves obtained from LSR-treated and untreated alloy, in order to analyses effects of LSR-treated on the corrosion resistance.

Figure 5 shows results of electrochemical polarization measurements of the laser-treated and untreated specimens. At open circuit potential (Ecorr), the corrosion current density (icorr) of the untreated and laser-treated specimens was calculated, equal to $9.73x10^{-7}$ A/cm^2 and $9.95x10^{-6}$ A/cm^2, respectively. This means in ten-fold decrease the corrosion current for laser-treatment sample. This fact can be considered due to the presence of Al_2O_3 and AlN phases, in most of diffraction peaks of treated sample (Figure 2).

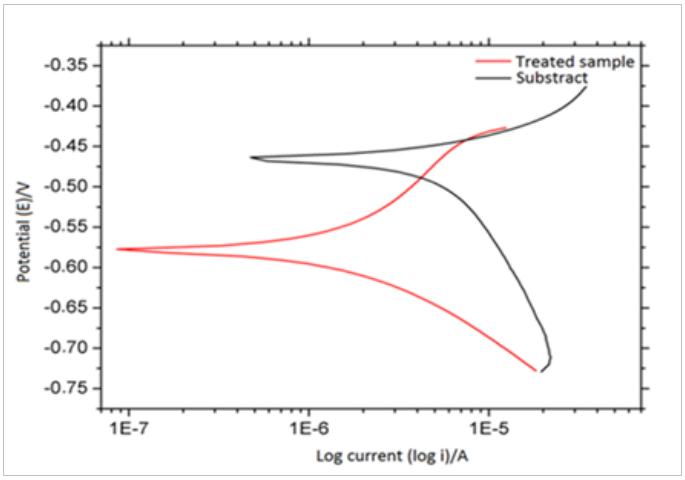

Figure 5 Effect of LSR-treated and untreated alloy under application of Tafel plots during immersion in 0.1 mol/L of H_2SO_4 at 25°C.

As a consequence of application of open-circuit corrosion potential, linear micropolarization and anodic polarization curves and result is summarized in Table 1, where are shown electrochemical parameters for Al–2.0 wt.% Fe alloy LSR-treated and untreated. Where, Ecorr is the open circuit potential, Rp is the polarization resistance, βA and βC anodic and the cathodic Tafel constants, and Icorr is the corrosion current density.

According to result of Table 1, electrochemical parameters that correspond to the material LSR-treated showed better results than the untreated material.

Cyclic voltammetry technique

Electrochemical methods make use of measurable electrical properties (current electrical, potential differences, accumulation interfacial charge, among others), from phenomena in which a redox species interacts, physically and / or chemically with other components of medium, or even with interfaces. Luther et al.,[20] pointed out, that efficiency of cyclic voltammetry technique, result of its feature to provide rapid information on thermodynamics of redox processes, of heterogeneous reaction kinetics of electron transfer and on chemical reactions coupled to adsorptive processes. Yet these same authors argue that, there are two main components, which determine the reactions, which occur in the electrode: diffusional mass transfer of analytic in a solution to electrode surface, and heterogeneous charge transfer between analytic and electrode. In some cases may occur chemical reactions coupled to any of these processes. Yet they affirm, Butler-Volmer equation is the basic equation of the electrochemical kinetics, which expressed these relationships.

A comparative study was carried out of cyclic polarization to laser-treated and untreated samples, with purpose of studying behavior of these materials in the same electrolyte solution. Figure 6 shows confrontation of cyclic polarizations curves for the laser-treated and untreated specimens, in aerated solution of H_2SO_4 0.1 molL^{-1}, at 25°C. Oxidation peaks and reduction peaks are no observed in both samples in the potential range shown in Figure 6, demonstrating that these reactions are of irreversible character at this condition.

Citation: Parionaa MM, Micene KT, Zaraa AJ. Corrosion behavior of Al-Fe alloy metastable phases produced by laser surface remelting technic. *Adv Tissue Eng Regen Med Open Access*. 2018;4(3):57–62. DOI: 10.15406/atroa.2018.04.00079

Table 1 Electrochemical parameters obtained for Al–2.0 wt.% Fe alloy LSR-treated and untreated sample in 0.1 mol/L H_2SO_4, performed by open-circuit corrosion potentials technic, linear micropolarization and anodic polarization curves

Region	Ecorr (V)	R_p (KΩ)	β_a (V/dec)	β_c (V/dec)	Icorr (A/cm²)	Corrosion rate (mm/year)
Treated Surface	-0.577	22.1	0.086	0.117	$9.37e^{-7}$	0.07
Untreated Substrate	-0.629	2.08	0.066	0.172	$9.95e^{-6}$	0.78

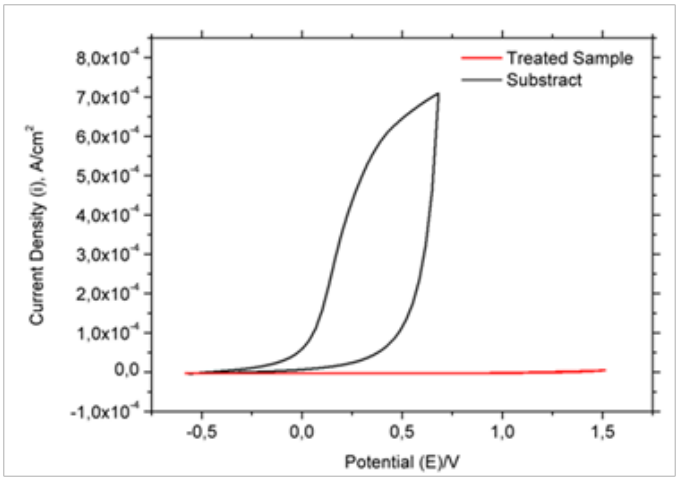

Figure 6 Cyclic voltammograms for LSR –treated and untreated samples.

The cyclic polarizations for the untreated specimen in H_2SO_4 aerated solution is shown in Figure 6 (black line). The cycle starts in −1.0V until the most anodic value +0.70 V, where in this potential the current density is about $6.5x10^{-4}$ A/cm², versus SCE, returning to −1.0 V, however the current density has a steady behavior, with low current density for LSR-treated sample in the same potential range. For untreated sample, during the anodic scan, current increase near of −0.10 V, associated with dissolution of aluminium, followed by formation of an aluminium oxide (Al_2O_3) film on the substrate. The anodic current rapidly increased until approximately +0.30 V, followed by a smaller growth rate until +0.70 V; it is characterized as a thickening region of oxide film. According to Kikuchi et al.,[21] potential increased linearly with anodizing time, due to formation of a anodic oxide film barrier, via following electrochemical reaction.

$$2Al + 3H_2O = Al_2O_3 + 6H^+ + 6e^-$$

With linear increase in the potential, the thickness of the barrier layer increased with anodizing time; in other words, the thickness increased with anodizing potential. After inversion potential, there is a sharp drop of the anodic current up to +0.50 V and, thereafter, reaching low values of currents in potential close to 0.0 V.

The cyclic polarization curve of Figure 6 (line red), it corresponds to laser-treated sample. The anodic current increases from potential +0.5 V as can be appreciated, this can be associated with growth of the aluminium oxide film and/or Al–Fe phases on the laser-treated surface, which is constituted by different phases, such as Al_2O_3, AlFe, $AlFe_3$ and $Al_{13}Fe_4$ and AlN, this was confirmed by X-ray (Figure 2). In the cyclic polarization curve, cycle starts in −1.0 V until the most anodic value +1.6 V, where the current density is about $0.2x10^{-6}$ A/cm² in +0.7 V. Result in 0.7 V, mean that the current density that corresponds to LSR-treated sample is much lower than untreated sample, being around 3 times.

According to this result, LSR-treated sample showed clearly the passive zone, then, LSR-treated sample results in reduction of the current density, and this fact indicates a lower corrosion rate, therefore, improvement corrosion resistance, this fact can be verified otherwise, the corrosion rate according to Table 1 was reduced by 11 times for LSR-treated sample, compared to untreated sample. According to previous discussion, LSR-treated sample surface was modify drastically, therefore, electrochemical corrosion behavior at 0.1 mol /L H_2SO_4 was propitiate passivity on the LSR-treated sample surface, reducing so the corrosion phenomena.

Conclusion

According to this study, following conclusions were made:

a. The melted zone is mainly due to high cooling rate imposed during LSR-treatment sample,

b. The melted zone was constituted of metastable phases by LAXRD analysis that revealed the presence mainly of Al_2O_3 and AlN phases. These phases contributed in microstructural modification, favored the characteristics of high hardness and corrosion resistance of LSR-treated sample in sulfuric acidic.

c. The polarization resistance has been increased about 11 times for the laser-treated sample relative to the untreated sample, implying directly on material corrosion resistance.

d. In cyclic voltammograms technique the reduction and oxidation reverse peaks/waves were not observed in both samples in the same potential range and so demonstrating that these reactions are of irreversible character at this condition.

e. LSR-treated sample showed clearly a wide passive zone, in ten-fold decrease the corrosion current after laser-treatment had occurred. However, LSR-treated sample acts in improvement corrosion resistance.

f. Electrochemical parameters that correspond to LSR-treated material showed better results than untreated material, therefore, this type of laser-treated alloy can be applied in aerospace, aeronautic, automobilist industries and implant material in humans.

g. To better understand more the efficiency of treated material laser. Other studies are being carried out such as, microhardness, study of roughness by atomic force technique, electrochemical impedance spectroscopy, Raman spectroscopy and numerical simulation by finite element using the Marangoni phenomenon and optimized by Multigrid technique.

Citation: Parionaa MM, Micene KT, Zaraa AJ. Corrosion behavior of Al-Fe alloy metastable phases produced by laser surface remelting technic. *Adv Tissue Eng Regen Med Open Access*. 2018;4(3):57–62. DOI: 10.15406/atroa.2018.04.00079

Acknowledgments

This work was entirely financed by CNPq (Brazilian National Council for Scientific and Technological Development), Fundação Araucária (FA), CAPES (Federal Agency for the Support and Evaluation of Postgraduate Education), and FINEP (Research and Projects Financing Agency). We also thank to LABMU–UEPG.

Conflict of interest

The author declares no conflict of interest.

Reference

1. Nakajima D, Kikuchi T, Natsui S, et al. Fabrication of a novel aluminum surface covered by numerous high-aspect-ratio anodic alumina nanofibers. *Applied Surface Science*. 2015;356:54–62.
2. Lee SJ, Park C, Lim YS, et al. Influences of laser surface alloying with niobium (Nb) on the corrosion resistance of Zircaloy-4. *Journal of Nuclear Material*. 2003;321(2-3):177–183.
3. Riva R, Lima MSF, Rodrigues NAS, et al. Using an Ytterbium fiber laser to fracture splitting of compacted graphite iron bearing caps. Proceedings of the Fourth International WLT-Conference on Lasers in Manufacturing. Munich; 2007;65–70.
4. Steen WM, Mazumder J. *Laser Material Processing*. 4th ed. New York: Springer; 2010:558.
5. Pariona MM, Teleginski V, dos Santos K, et al. Yb-fiber laser beam effects on the surface modification of Al Fe aerospace alloy obtaining weld filet structures, low fine porosity and corrosion resistance. *Surface Coating Technology*. 2012;206(8-9):2293–2301.
6. Pariona MM, Teleginski, dos Santos V, et al. AFM study of the effects of laser surface remelting on the morphology of Al–Fe aerospace alloys. *Materials Characterization*. 2012;74:64–76.
7. Sun Z, Annergren I, Pan D, et al. Effect of laser surface remelting on the corrosion behavior of commercially pure titanium sheet. *Materials Science and Engineering A*. 2013;345(1-2):293–300.
8. Pariona MM, Teleginski V, dos Santos K, et al. Influence of laser surface treated on the characterization and corrosion behavior of Al–Fe aerospace alloys. *Applied Surface Science*. 2013;276:76–85.
9. Yan C, Hao L, Hussein A, et al. Microstructure and mechanical properties of aluminium alloy cellular lattice structures manufactured by direct metal laser sintering. *Materials Science & Engineering A*. 2012;628:238–246.
10. Olakanmia EO, Cochranea RF, Dalgarno KW, et al. A review on selective laser sintering/melting (SLS/SLM) of aluminium alloy powders: Processing, microstructure, and properties. *Progress in Material Science*. 2015;74:401–477.
11. Fu B, Qin G, Meng X, et al. Microstructure and mechanical properties of newly developed aluminum–lithium alloy 2A97 welded by fiber laser. *Materials Science & Engineering A*. 2014;617:1–11.
12. Bertelli F, Meza ES, Goulart PR, et al. Laser remelting of Al–1.5wt.% Fe alloy surfaces: numerical and experimental analyses. *Optics and Lasers in Engineering*. 2011;49(4):490–497.
13. Olson DL, Siewert TA, Liu S. *ASM Handbook. Welding, Brazing and Soldering*. Materials Park, USA: ASM International; 1993.
14. Bian HM, Yang Y, Wang Y, et al. Alumina-titania ceramics prepared by microwave sintering and conventional pressure-less sintering. *Journal of Alloys and Compounds*. 2012;525:63–67.
15. Patnaik P. *Handbook of Inorganic Chemicals*. Burlington NJ: McGraw-Hill; 2003.
16. Gremaud M, Carrard M, Kurz W, et al. The microstructure of rapidly solidified Al-Fe alloys subjected to laser surface treatment. *Acta Metallurgia et Materialia*. 1990;38(12):2587–2599.
17. Li C, Wang Y, Guo L, et al. Laser remelting of plasma-sprayed conventional and nanostructured Al_2O_3–13wt.% TiO_2 coatings on titanium alloy. *Journal of Alloys and Compounds*. 2010;506(1):356–363.
18. Peyre P, Scherpereel X, Berthe L, et al. Surface modifications induced in 316L steel by laser peening and shot-peening. Influence on pitting corrosion resistance. *Materials Science and Engineering A*. 2000;280(2):294–302.
19. Khalfaoui W, Valerio V, Masse JE, et al. Excimer laser treatment of ZE41 magnesium alloy for corrosion resistance and microhardness improvement. *Optics and Lasers in Engineering*. 2010;48(9):926–931.
20. Lutheu GW, Glazer BT, Ma S, et al. Use of voltammetric solid-state (micro)electrodes for studying biogeochemical processes: Laboratory measurements to real time measurements with an in situ electrochemical analyzer (ISEA). *Marine Chemistry*. 2008;108(3-4):221–235.
21. Kikuchi T, Nakajima D, Kawashima J**.** Fabrication of anodic porous alumina via anodizing in cyclic oxocarbon acids. *Applied Surface Science*. 2014;313**:**276–285.